



Supplementary Materials for

A Cascade of Histone Modifications Induces Chromatin Condensation in Mitosis

Bryan J. Wilkins, Nils A. Rall, Yogesh Ostwal, Tom Kruitwagen, Kyoko Hiragami-Hamada,
Marco Winkler, Yves Barral, Wolfgang Fischle, Heinz Neumann*

*Corresponding author. E-mail: hneumann@uni-goettingen.de

Published 3 January 2014, *Science* **343**, 77 (2014)
DOI: 10.1126/science.1244508

This PDF file includes:

Materials and Methods

Figs. S1 to S17

Tables S1 to S3

References

Materials and Methods

Standard yeast genetic manipulation

All strains and primers used in this study are listed in Supplementary Tables S1 & S2. The *S. cerevisiae* histone H2A (HTA1) gene, including 450 bp up/downstream of the ORF, was cloned from yeast genomic DNA as a SacI/XhoI PCR fragment into pRS426 (27). An HA epitope coding sequence was introduced just prior to the stop codon using standard QuikChange protocol. Site-specific amber codon mutations were also introduced through standard QuikChange methods. The expression vectors were co-transformed into yeast cells with the plasmid pESC-BPARS, which harbors the evolved *E. coli* Tyr-tRNA_{CUA}/AARS pair, under control of constitutive promoters, specific for pBPA incorporation (15). All yeast transformations were performed by standard lithium acetate/heat shock methods.

BY4741 *alk1/alk2Δ* strain was established through genomic integration of the HIS3 gene at the *alk1* locus in BY4741 *alk2Δ::KanMX*. Standard PCR amplification of the pRS303 plasmid was performed to amplify the HIS3 region with flanking sequences to the *alk1* ORF. The PCR products were ethanol precipitated and then transformed into *alk2Δ* cells. Genomic integration was selected against histidine SC dropout agar and surviving colonies were streaked through two rounds on histidine SC agar. The initial *alk2Δ* strain and the double knockout *alk1/alk2Δ* were verified by yeast genomic DNA extraction and PCR.

Yeast cultures and crosslinking

Histone H2A expression vectors with the appropriate amber mutations, under control of their native promoter, were co-transformed into yeast cells with the plasmid pESC-BPARS, which harbors the evolved *E. coli* Tyr-tRNA_{CUA}/AARS pair, under control of constitutive promoters (15). In all experiments, yeast cells were cultured in the appropriate standard synthetic complete (SC) dropout medium (1.7 g/L Difco Yeast nitrogen base without amino acids, 5 g/L ammonium sulfate, 2% glucose, and 2 g/L amino acid dropout mixture). Cells were grown at 30°C with shaking at 210 rpm, unless otherwise noted. For cells expressing full-length pBPA mutants, media was supplemented with 1 mM pBPA final concentration. Cultures were initiated at OD₆₀₀ ~0.2 from an overnight culture and the cells were collected in late exponential phase. Whole cell lysates were normalized to 12 OD units and resuspended in 100 μL SC medium on ice for UV treatment. Live cells were exposed to 365 nm UV light at a distance of ~5 cm for 7 min on ice (Vilber Lourmat lamp, 2 X 8W, 365 nm tubes, 32 W, 230 V #VL-208.BL). Lysates were prepared by incubating cells in 200 μL 100 mM NaOH for 10 min at room temperature. Cells were collected and then resuspended in 100 μL preheated 2xSDS loading buffer at 95°C, and boiled for 10 min. Lysates were clarified and then loaded on SDS-PAGE gels for Western blot analysis.

The formation of crosslink products depended on irradiation with UV light (fig. S15). Cells encoding pBPA in the presence of H2A-HA lacking amber codons, did not produce crosslink products, demonstrating the specificity of the crosslinking experiments (fig. S16). Separation of cytosolic and chromatin bound fractions after crosslinking verified that the majority of crosslinks emanate from nucleosomal histones (fig. S17).

Recombinant xIH2A-pBPA, Array reconstitution, condensation and crosslinking

Recombinant xIH2A with pBPA at position Y57 or E64 was prepared using pCDF xIH2A containing the gene for *X. laevis* H2A optimized for expression in *E. coli* and an amber codon at the appropriate position. The plasmid was used to express His-tagged xIH2A in the presence of pSUP-BPARS (28) in *E. coli* BL21 DE3 in the presence of 1 mM pBPA. Expression was induced at OD₆₀₀ ≥ 1 by addition of 1 mM IPTG. The protein was purified and processed into histone octamers as described (29).

25 µg 12x601-200 DNA was mixed with WT or xIH2A-pBPA-containing histone octamers at 1:1.1 molar ratio and nucleosomal arrays were reconstituted by salt dialysis. 1 µg (according to A₂₆₀) of arrays was diluted in 100 µl TEA buffer (10 mM Triethanolamine-HCl pH 7.5, 0.1% Triton-X100, 0.1 mM EDTA) with or without 5 mM MgCl₂ and incubated for 30 min on ice. Arrays were then irradiated with UV (365 nm) three times for 10 min on ice. After UV irradiation, 5 mM MgCl₂ was added to 'no salt' samples. All samples were centrifuged at 16.1k x g for 30 min at 4°C to precipitate arrays. The pellets were dissolved in 15 µl 1x SDS loading buffer and analyzed by SDS-PAGE and subsequent Western blotting with anti-H4 antibody.

MNase digest of nucleosome arrays

5 µg/ml WT or xIH2A-pBPA arrays were incubated with 0.2 U/ml Boehringer MNase (Takara) in MNase buffer (20 mM Tris-HCl pH 8.0, 5 mM NaCl, 2.5 mM CaCl₂) at 37°C for 0, 30 s, 2 min, or 15 min. At each time point, 100 µl of the reaction were mixed with 200 µl buffer NTI from Macherey-Nagel Nucleospin Gel and PCR clean-up kit to quench the reaction. DNA was purified using the clean-up kit according to the manufacturer's instructions. The purified samples were analyzed by agarose gel electrophoresis.

Western blot analysis

Proteins were separated by SDS-PAGE and transferred to PVDF membrane at a constant 100 V for 1.5 h at 4°C. Transfer was done in standard Tris-glycine buffer containing 0.1% SDS. Primary and secondary antibody binding was performed as indicated in Table S3. All blots were washed with TBS + 0.1% Tween-20 for 5 min following secondary antibody incubation. All secondary antibodies were HRP conjugated and detection was performed via chemo-luminescence (Pierce ECL plus, # 32132). All quantification of blots was performed using ImageJ. Anti-HA crosslinked bands were normalized to bulk H2A-HA signal from each time assayed. For H4 reactive antibodies, the crosslink was normalized to the bulk H4 signal.

Cellular Fractionation

BY4741 cells with the appropriate pBPA mutants were fractionated as previously reported (30). In brief, 50 mL of cells were collected at an OD = 1.2. The cells were resuspended in 10 mL of growth medium for treatment with UV light (as described above). The cells were washed in PSB buffer (20 mM Tris-HCl, pH 7.5, 2 mM EDTA, 100 mM NaCl, 10 mM β-ME), then SB buffer (1 M sorbitol, 20 mM Tris-HCl, pH 7.5), and then resuspended in 1 mL of SB with 50 U/mL lyticase (Sigma L2524). Cells were incubated at RT with slight shaking until the OD was lessened by more than 85% (~1 h). Spheroblasts were washed with SB buffer, and then resuspended in 0.5 mL EBX buffer (20 mM Tris-HCl, pH 7.5, 100 mM NaCl, 0.25% Triton X-100, 15 mM β-ME, 50 mM

Na-butyrate, 1× protease inhibitor cocktail, and 1 mM PMSF). Triton X-100 was added to a final concentration of 0.5% and the samples were incubated at 4°C for 10 min with slight shaking (whole cell fraction). The lysate was layered over 1 mL NIB buffer (20 mM Tris-HCl, pH 7.5, 100 mM NaCl, 1.2 M sucrose, 15 mM β -ME, 50 mM Na-butyrate, 1× PIC protease cocktail, and 1 mM PMSF) and then centrifuged at 17K x g for 15 min at 4°C. The cytoplasmic fraction remained in the upper layer. The nuclear pellet was resuspended in 0.5 mL EBX with Triton X-100 added to 1% final concentration, and incubated at 4°C for 10 min with slight shaking. The chromatin fraction was collected by centrifugation at 17K x g for 10 min at 4°C. The pellet was washed three times with EBX and resuspended in 50 μ L of 1 M Tris-HCl, pH 8.0. Each fraction was treated with SDS loading buffer and analyzed by SDS-PAGE and subsequent blotting.

Immunoprecipitation

W303 cells harboring the appropriate pBPA mutants were grown in 2 L of SC medium overnight. Control cells contained a suppression system using a wild-type *E. coli* tyrosyl-tRNA synthetase, recognizing native cellular tyrosine instead of pBPA. Cells were collected the next day ($3.0 < OD_{600} < 4.0$) and resuspended in 10 mL of growth media for UV treatment. Lysis of cells was performed in PBS buffer supplemented with 1×PIC and 1 mM PMSF (1:1 PBS to cell pellet v/v) by flash freezing in liquid nitrogen and disruption by ultra centrifugal rotor mill (Retsch ZM200, # 20.823.0001). Triton-X 100 was added to the lysates to 1% final concentration and then clarified by centrifugation at 39K x g for 30 min at 4°C. The pellet was washed twice in PBS and collected by centrifugation. The insoluble proteins were resuspended in 1 mL DMSO and incubated at 37°C with shaking for 1 h. After one hour, 30 mL of extraction buffer (7 M Guanidinium-HCl, 20 mM Tris-HCl pH 7.5, 10 mM DTT) was added, mixed thoroughly by vortexing, and incubated at RT with rotation for 2 h. The extracted proteins were clarified by centrifugation at 39K x g for 30 min at 4°C. The supernatant was then dialyzed against urea buffer (7 M Urea, 10 mM Tris-HCl, pH 8.0, 1 mM EDTA, 0.1 M NaCl, 5 mM β -ME) and histone proteins were subsequently isolated by ion exchange (GE HiTrap SP, 5 ml, # 17-1151-01) in urea buffer with 100 mM NaCl and eluted in urea buffer with 1 M NaCl. The elution fraction was concentrated to 1.5 mL and diluted 5 times with IP buffer (15 mM Na_2HPO_4 , pH 7.5, 150 mM NaCl, 2% Triton X-100, 0.1% SDS, 0.5% w/v Na- deoxycholate, 10 mM EDTA). IP reactions were performed with anti-HA agarose (Pierce, #26182) for 2 h at 4°C. Beads were washed once with IP buffer, twice with PBS, once with PBS (300 mM NaCl) and eluted in 1×SDS loading buffer.

Cell cycle arrest and release

α -Factor synchronizations were performed in BY4741 cells expressing H2A-pBPA mutants. An overnight culture of 200 mL in SC medium (supplemented with 1 mM pBPA) was diluted to an $OD_{600} = 0.2$ in 200 mL YPDA and incubated for 2 h, with shaking, at 30°C. α -Factor (Sigma T6901) was added to a final concentration of 5 μ g/mL. Cells were monitored by microscopy until >95% of cells arrested in the G1 phase “schmoo” morphology. Following arrest the cells were washed twice with 400 mL YPDA and released into YPDA at an $OD_{600} = 0.4$, 30°C. Samples were taken at indicated time points, treated with UV, and analyzed by Western blot.

Nocodazole arrest was performed in BY4741 cells containing the appropriate H2A mutants at 30°C. An overnight culture of 200 mL in SC medium (supplemented with 1 mM BPA) was back diluted to an OD₆₀₀ = 0.4 in 500 mL YPDA and incubated for 2 h with shaking. This culture was diluted again to OD₆₀₀ = 0.4 in YPDA. Nocodazole was added to a final concentration of 15 µg/mL from a 100X stock solution (1.5 mg/mL in DMSO). Cells were returned to 30°C with shaking for 1.5 h for complete arrest (as determined by FACS analysis (31)). Release of cells was performed with excessive washing (4 times 500 mL YPDA + 1% DMSO). Released cells were returned to shaking at 30°C and samples were taken at specific time points, treated with UV, and analyzed by Western blot.

Nuclei isolation and histone extraction

Yeast nuclear fractions were isolated and subjected to acid extraction as modified from (32). In brief, cells were cultured as described above, where nuclei were isolated from 100 OD units in exponential growth. Cells were incubated in Tris-HCl, pH 7.5, containing 30 mM DTT, at 30°C for 10 min, with shaking. The cells were collected at 5K x g and spheroplasts were prepared by incubating the cells in lyticase buffer (YPD medium containing 1 M sorbitol, 100 U/mL lyticase, 1 mM DTT, 1X PIC, 10 mM sodium butyrate, and 1 mM PMSF) with gentle shaking at 30°C for 20-30 min (monitored visually by “ghosting” in 1% SDS under microscope). Spheroplasts were collected at 3K x g and washed once in YPD plus sorbitol, 4°C, and then washed again with ice cold 1 M sorbitol. The spheroplasts were resuspended in 5 mL nuclear isolation buffer (NIB, 10 mM Tris-HCl, pH 7.5, 18% Ficoll-400, 20 mM KCl, 1 mM EDTA, 0.15 mM spermine, 0.5 mM spermidine, 1X PIC, 10 mM sodium butyrate, and 1 mM PMSF) and then lysed by douncing 20 times, size S dounce. The nuclei were clarified by centrifugation at 3K x g and the resulting supernatant was removed. The nuclei in the supernatant were collected by centrifugation at 16.5K x g, where the nuclear pellet was then resuspended in 400 µL 0.4 N H₂SO₄, and vortexed repeatedly for 30 min, on ice. The acid extractions were set on a rotator, over night at 4°C. The nuclear remnants were removed from the histone extraction by centrifugation at 16.5K x g. The resulting supernatant, containing the histones, was then precipitated by adding 100% TCA to a final concentration of 33% (v/v), and set on ice for 2 h. The histones were collected at 16.5K x g and washed twice with ice cold acetone. The histones were allowed to air dry and then diluted in 100 µL 20 mM Tris-HCl, pH 8.0.

Pull-downs

30 µl 50:50 slurry of Pierce® Avidin Agarose Resin were washed three times with PBS (1 min incubation in buffer followed by centrifugation with 500 x g at 1 min). 10 µg of histone peptide (residues 1-20: NH₂-ARTKQTARKS(unmodified or phosphorylated)TGGKAPRKQL-K(biotin)-CONH₂) were added and the samples were incubated for 3 h at RT while shaking (1400 rpm). Unbound peptides were removed by three washing steps (as before). Genomically encoded GFP-tagged *HST2* or *SIR2* yeast transgenic strains were subjected to Rotor mill lysis in TBS-T (0.5%) containing phosphatase inhibitor cocktail (Sigma). The lysate was spun at 15K x g for clarification. 2.5 mg of whole cell extracts were added to the peptide-coated beads and samples were incubated over night at 4°C under constant rotation. Beads were washed six times with 1

ml PD150 buffer (20 mM HEPES-NaOH pH 7.9, 150 mM KCl, 0.2% Triton® X-100, 20% glycerol) for 5 min at 4°C. Proteins recovered on the peptide-coated beads were eluted by boiling in SDS-PAGE loading buffer. Analysis was performed by Western blotting.

Microscopic hypercondensation assay

Yeast chromosome fusions and mutants were generated as described previously (4). For microscopy, cells were grown at 30°C in YPD and were placed on minimal synthetic medium agar pads and still images (taking stacks of 18 focal planes 0.5 µm apart) were taken using an applied Precision DeltaVision wide-field fluorescent microscope with a Roper CoolSnap HQ2 camera. Statistical t-tests (allowing for unequal variance) were performed using Prism software (GraphPad).

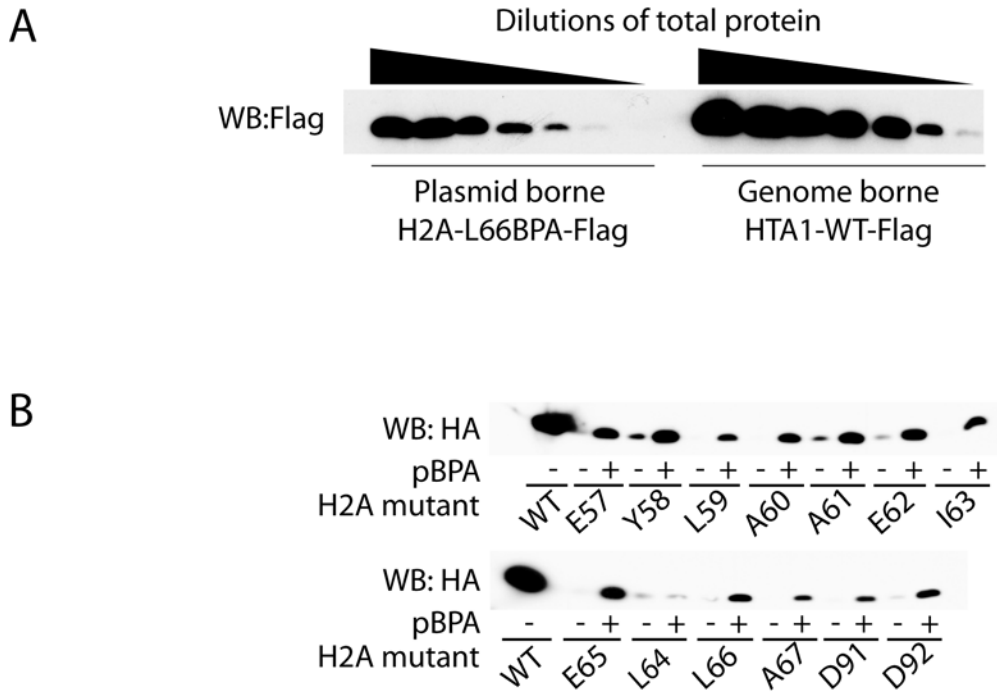


Fig. S1. A) Suppression of an amber codon in H2A (E66TAG) with pBPA produces approximately 10% of the endogenous amount of H2A. Dilution series of total protein (from left to right: 1:1, 1:2, 1:5, 1:10, 1:20, 1:50, 1:100) loaded from an H2A E66pBPA mutant expressed through an additional copy of HTA1 on a plasmid or from a yeast strain where one of the two H2A genes was replaced by HTA1-WT-FLAG was analyzed by SDS-PAGE and Western blotting with anti-FLAG antibodies. **B)** Amino acid dependency of full-length protein expression of H2A amber mutants. Cells were cultured in the presence and absence of pBPA to late exponential phase. Whole cell lysates were analyzed by SDS-PAGE and Western blot using anti-HA antibodies.

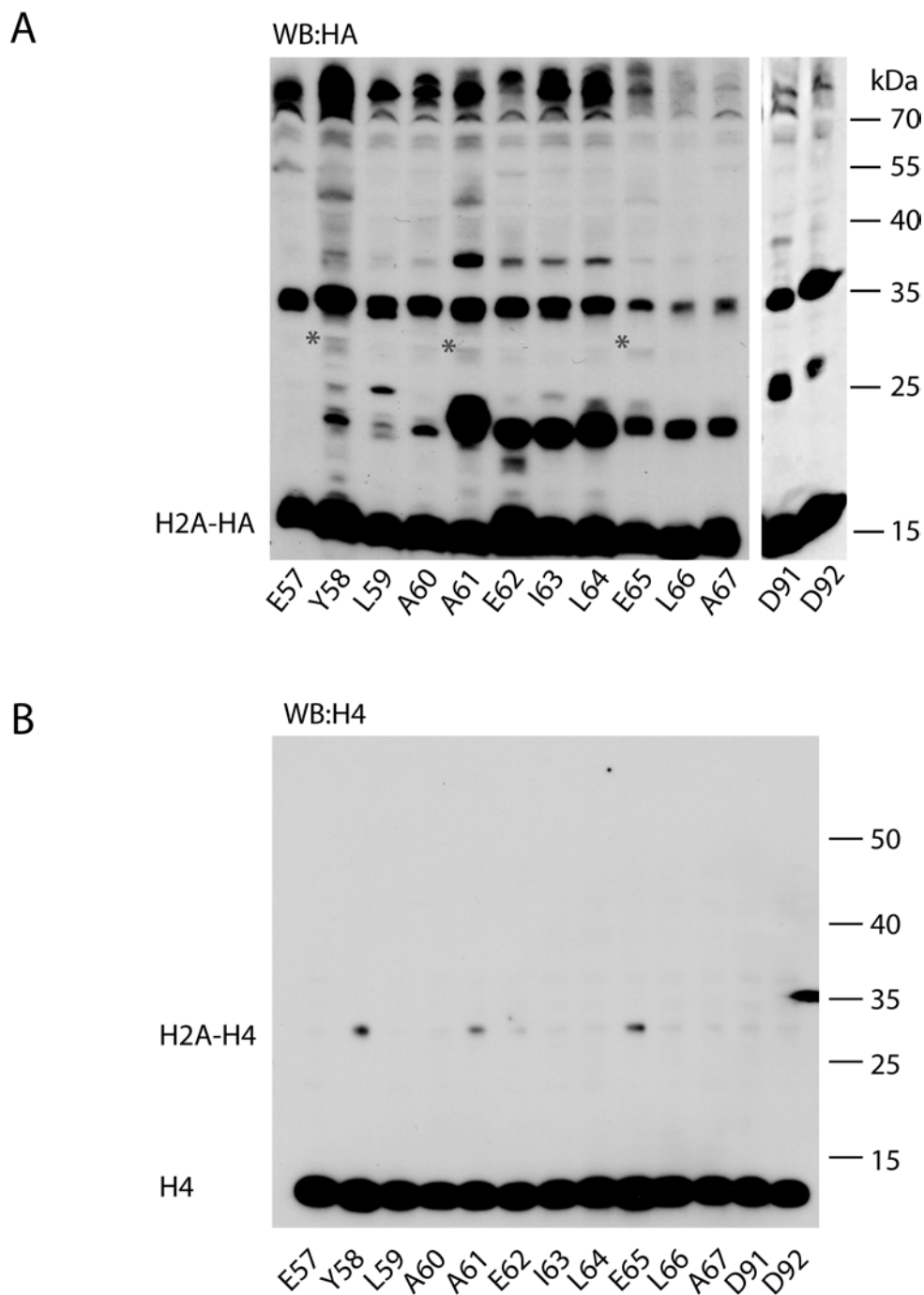


Fig. S2 Overview of crosslink products obtained from different sites along the acidic patch. **A)** Western blot analysis (anti-HA) of whole cell lysates from cells expressing H2A-HA with pBPA at the indicated positions. A crosslink band at ~30 kDa (*) matches a H2A-H4 interaction in mass. **B)** Acid-extracted nuclei of the same mutants as in **A** were analyzed using anti-H4 antibodies.

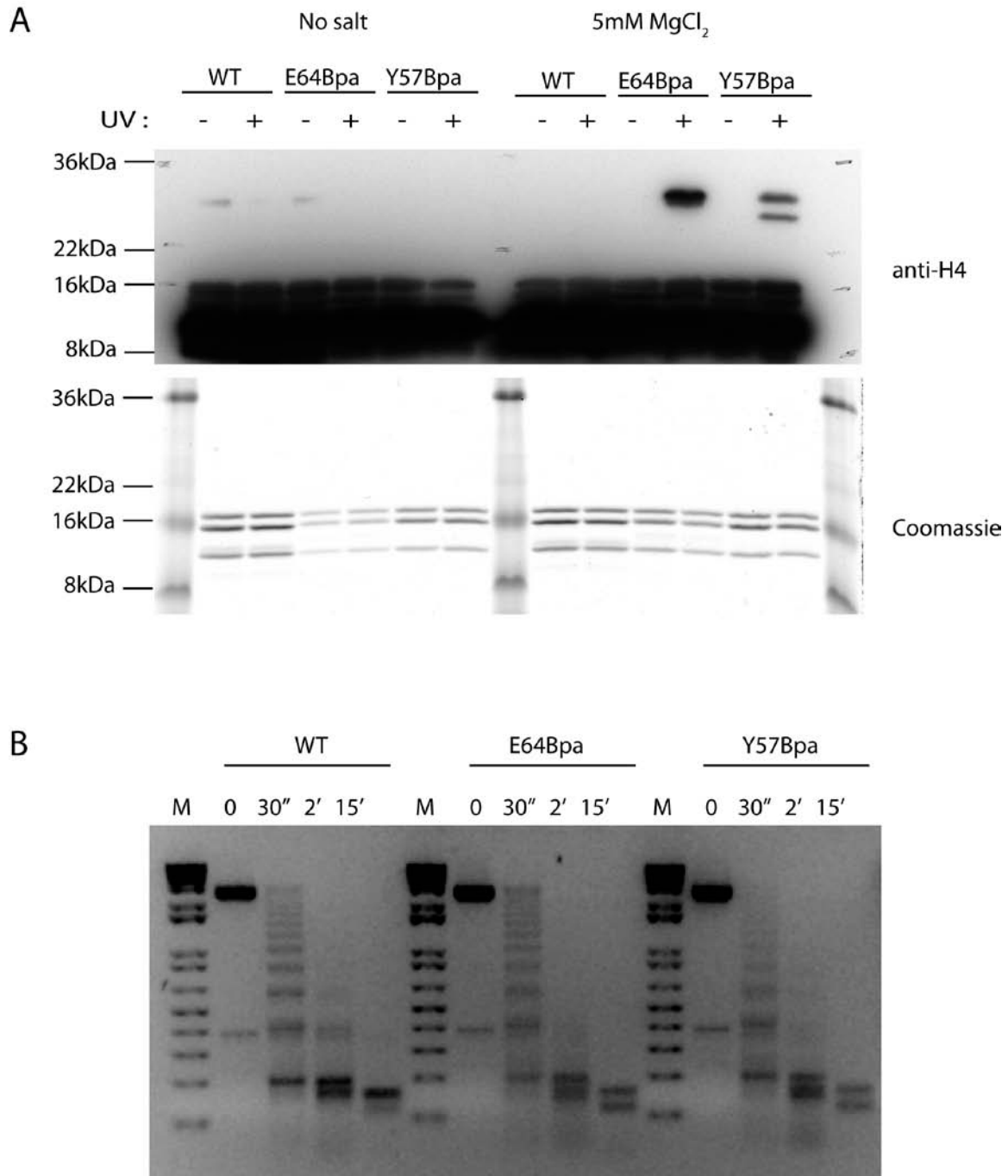
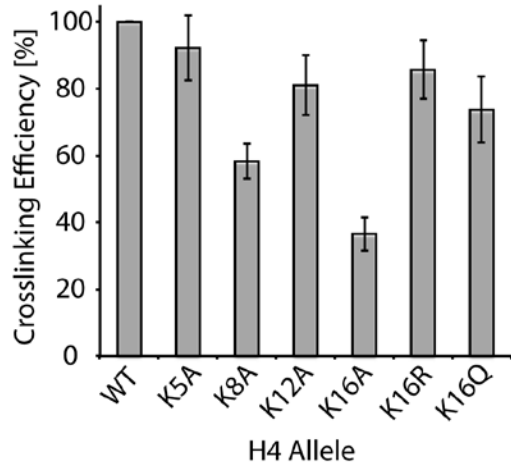
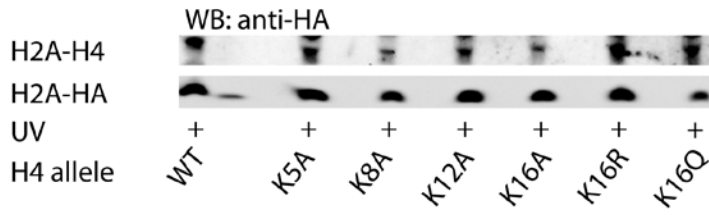
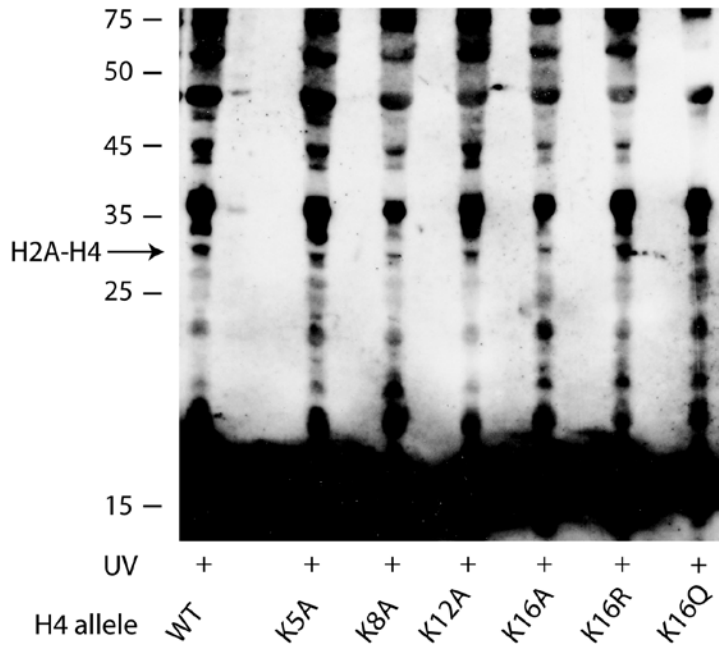


Fig. S3 Formation of the H2A-H4 crosslink product *in vitro* depends on array compaction. **A)** 12x601-200bp arrays of nucleosomes reconstituted using xIH2A with pBPA at the indicated positions were treated with UV in the presence or absence of 5 mM MgCl₂ and analyzed by Western blot with anti-H4 antibodies. **B)** MNase digest of arrays used in **A**.

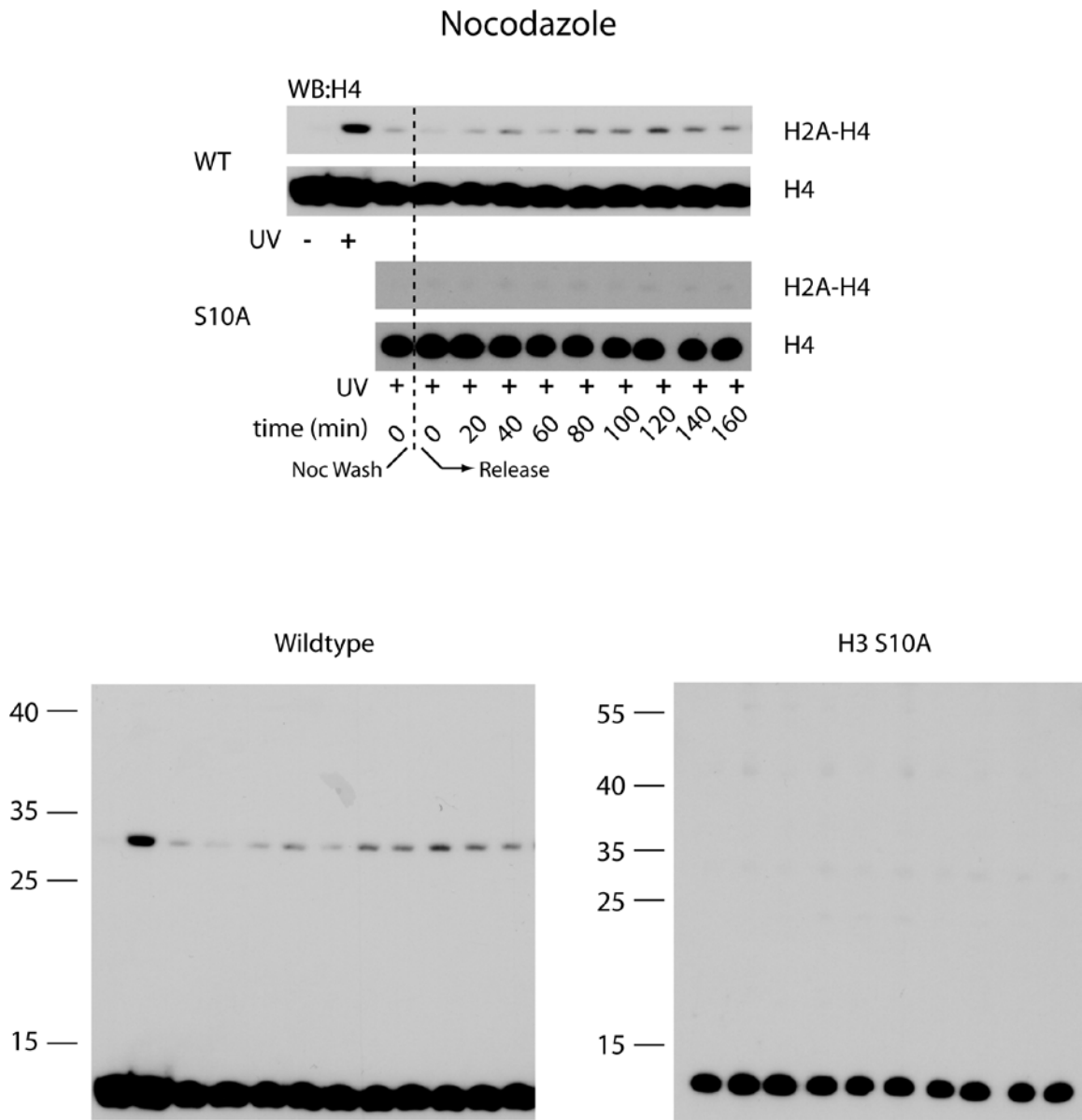


Densitometric analysis



Full-size Western blot

Fig. S4 Mutations in the H4 tail affect the interaction with the acidic patch. Yeast cells were treated as in Fig. 1C, crosslink products were analyzed in whole cell lysates using anti-HA antibodies and crosslinking efficiency quantified by densitometry using ImageJ (in three independent experiments, error bars represent standard deviation of the means).



Full-sized Western Blots to Figure above; anti-H4.

Fig. S5 The H2A-H4 interaction in mitosis depends on H3 S10. H3 S10A mutant or the corresponding wild-type cells expressing H2A Y58pBPA were synchronized using nocodazole. At the indicated times samples were taken, histones acid-extracted from isolated nuclei and analyzed by SDS-PAGE and Western blot using anti-H4 antibodies.

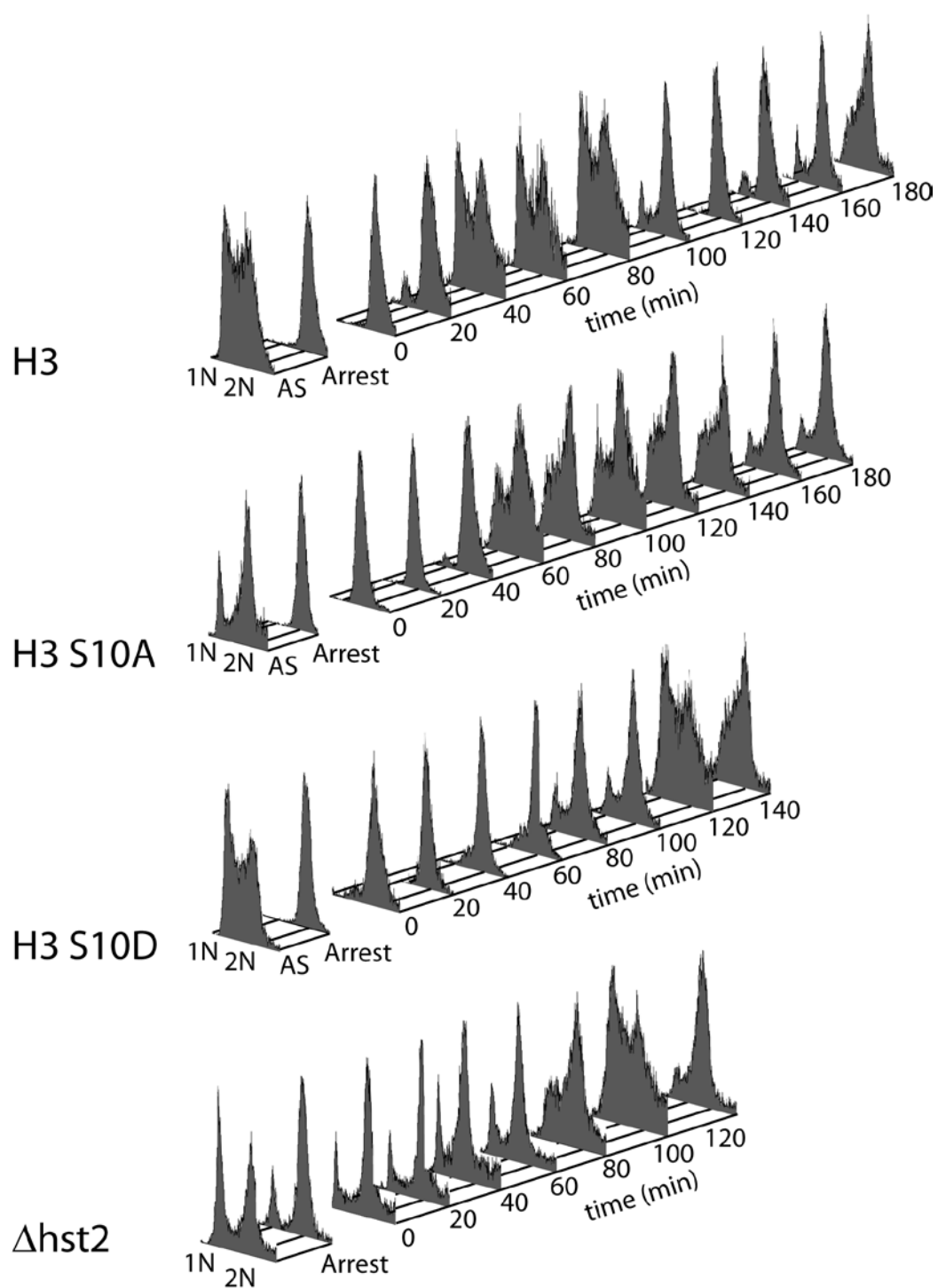


Fig. S6 FACS analysis of nocodazole-synchronized strains containing the indicated genomic alterations. The same samples were analyzed by Western blot in Figure 3B.

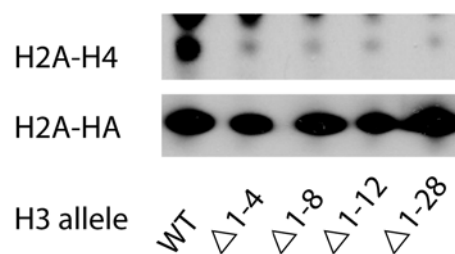


Fig. S7 Nocodazole synchronization (arrest) of Thermo Scientific Open Biosystems H3 and H4 non-essential histones collection. Cells containing genomic H4 mutations were transformed with plasmids to produce H2A-HA Y58pBPA then arrested in metaphase with nocodazole and treated with UV for 7 min on ice. Samples were analyzed by SDS-PAGE and Western blot using anti-HA antibody.

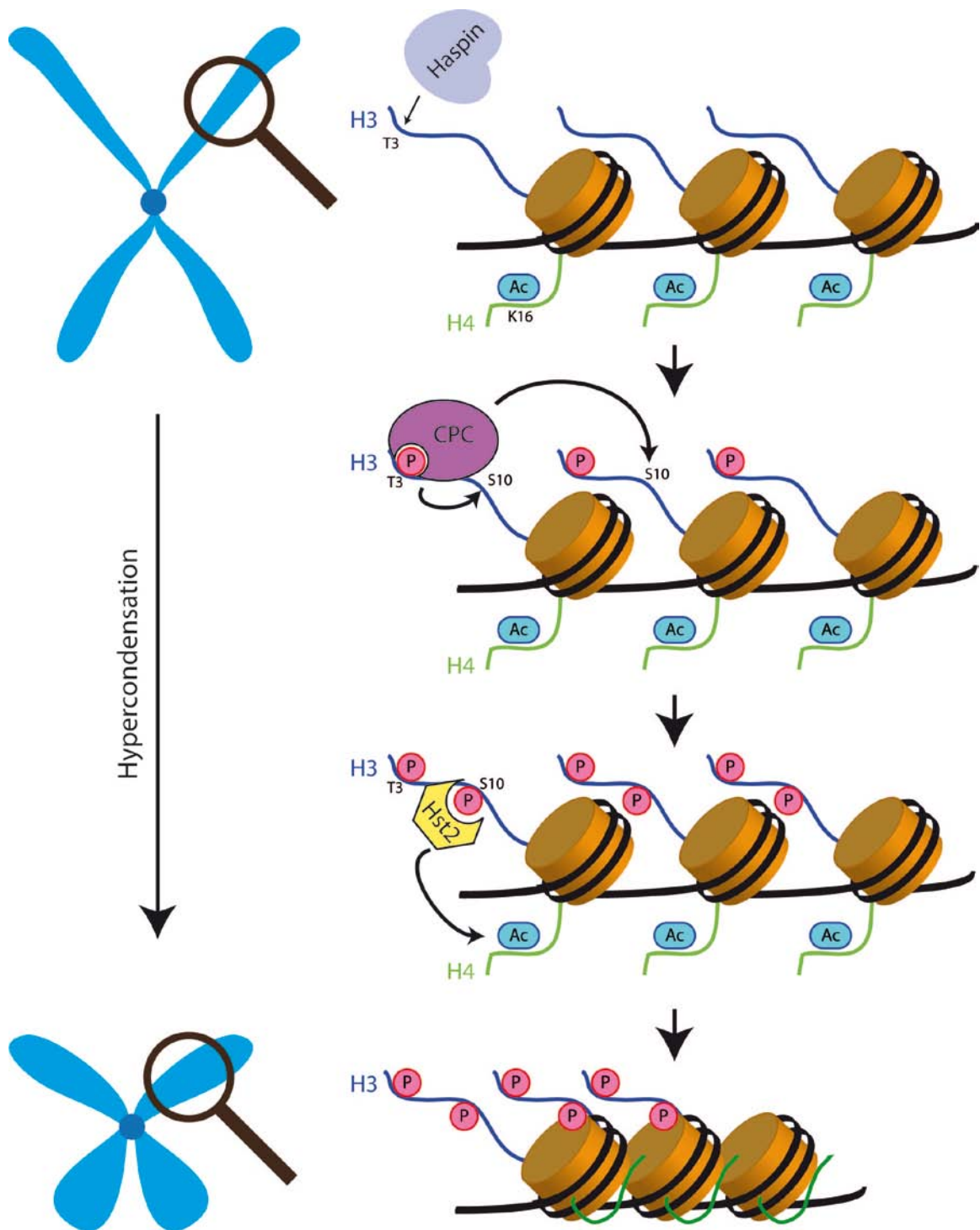


Fig. S8 Model of a cascade of histone modifications that activates H4-tail mediated mitotic chromatin condensation.

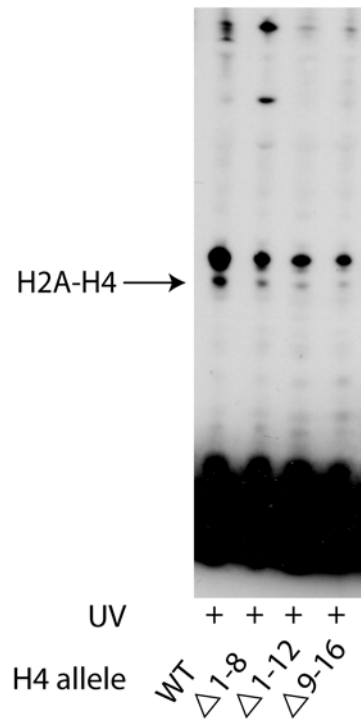


Fig. S9 Nocodazole synchronization (arrest) of Thermo Scientific Open Biosystems H3 and H4 non-essential histones collection. Cells containing genomic H4 mutations were transformed with plasmids to produce H2A-HA Y58pBPA then arrested in metaphase with nocodazole and treated with UV for 7 min on ice. Samples were analyzed by SDS-PAGE and Western blot using anti-HA antibody.

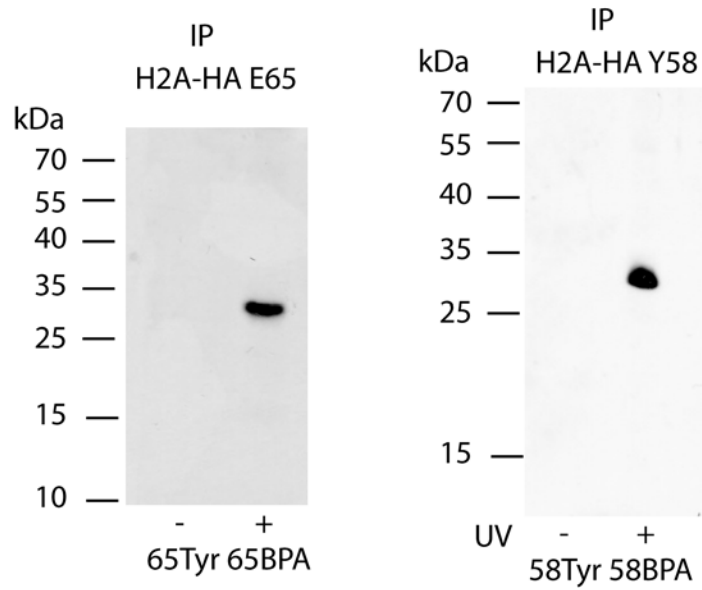


Fig. S10 Anti-HA immunoprecipitations from extracts containing Tyr or pBPA at the indicated positions of H2A-HA. Western blots were decorated using histone H4 antibodies. The signals at approximately 30 kDa match the size of a H2A-H4 crosslink.

α -factor synchronization

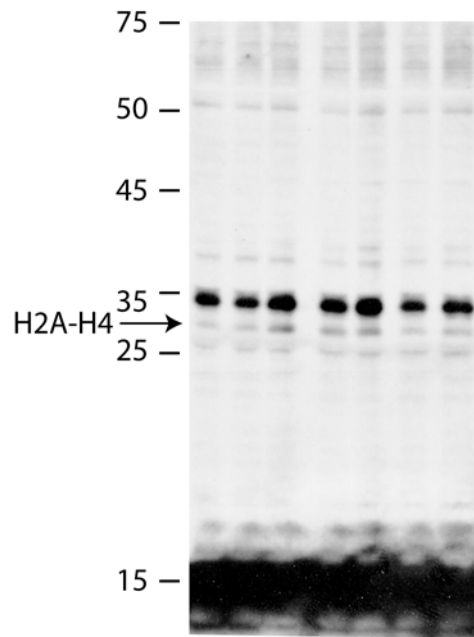


Fig. S11 Whole anti-HA decorated Western blot of the cell cycle arrest and release experiment shown in Figure 2A. The H2A-H4 band depicted in the main text figure is shown with an arrow.

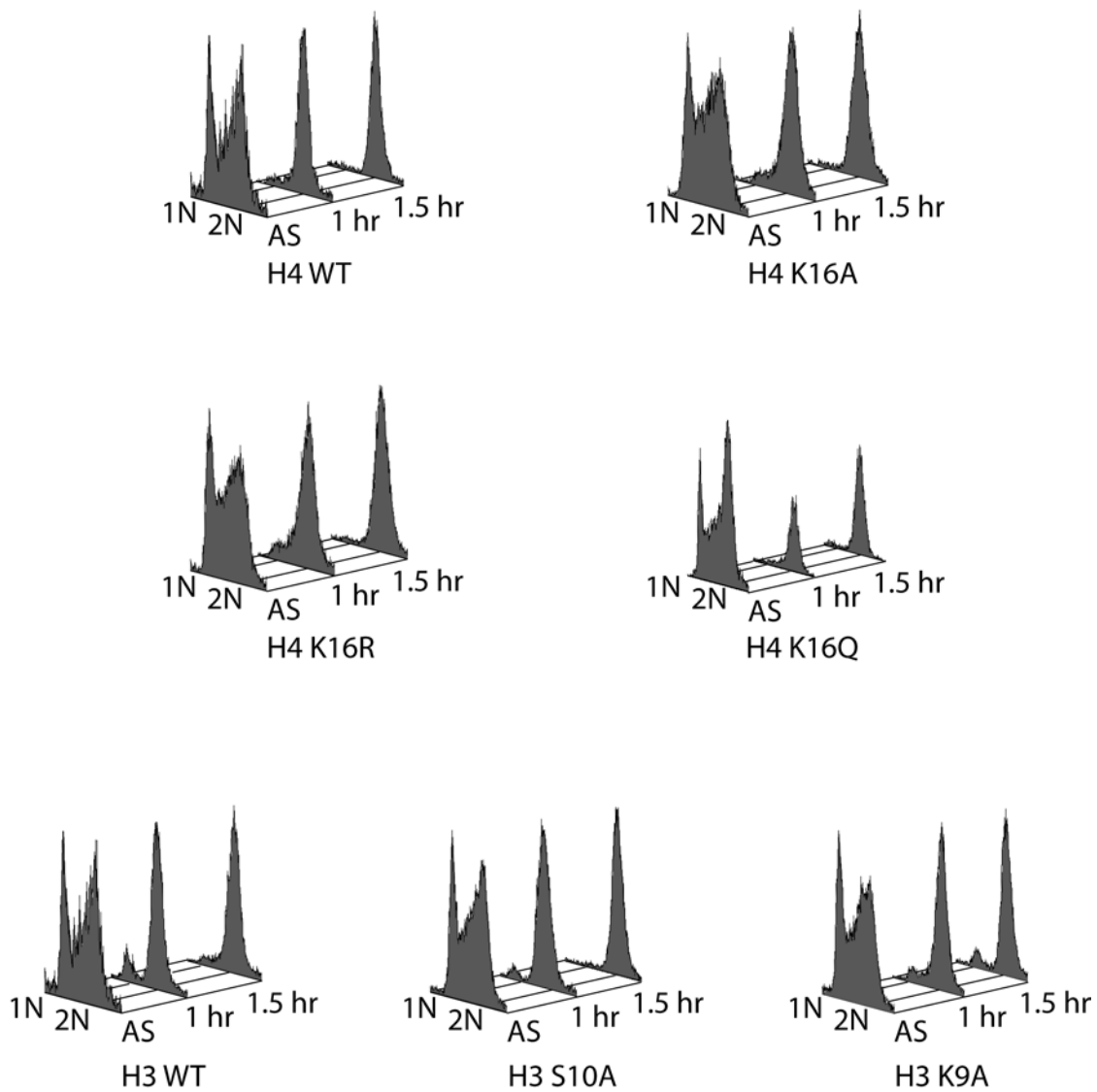


Fig. S12 FACS analysis of nocodazole synchronization of selected mutants of the Thermo Scientific Open Biosystems H3 and H4 non-essential histones collection. Complete synchronization occurs at 1.5 h after the addition of nocodazole. The presence of genomic mutations does not affect the percent of the population in arrest or the time required to reach arrest.

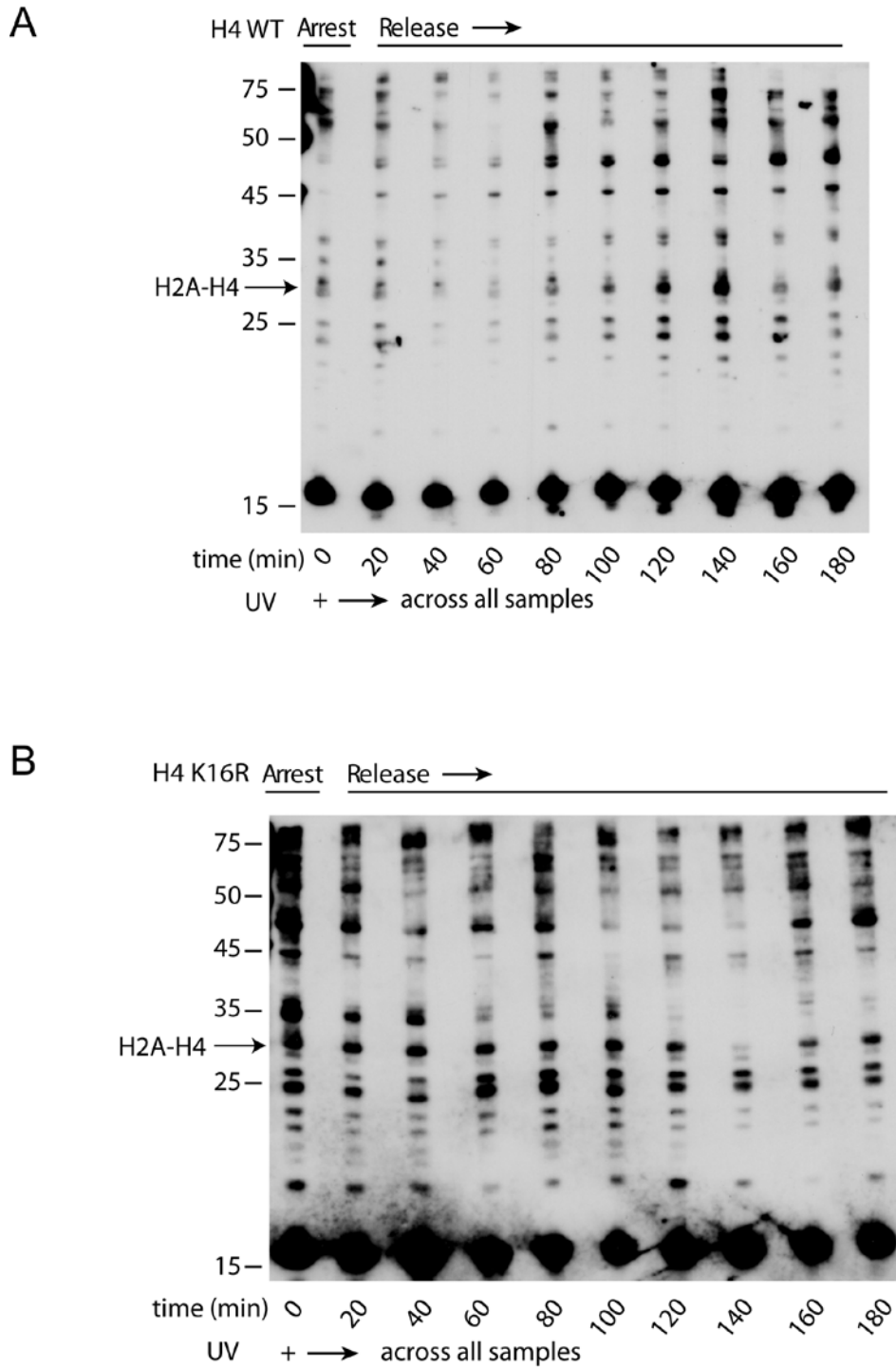


Fig. S13 Nocodazole synchronization (arrest and release) of H4 K16R mutant yeast cells. **A)** H4 WT cells were arrested in metaphase with nocodazole and synchronously released. Samples were taken after release and treated with UV for 7 min on ice, then analyzed by SDS-PAGE and Western blot using anti-HA antibodies. **B)** H4 K16R cells were arrested with nocodazole and synchronously released. Samples were treated as described in **A**.

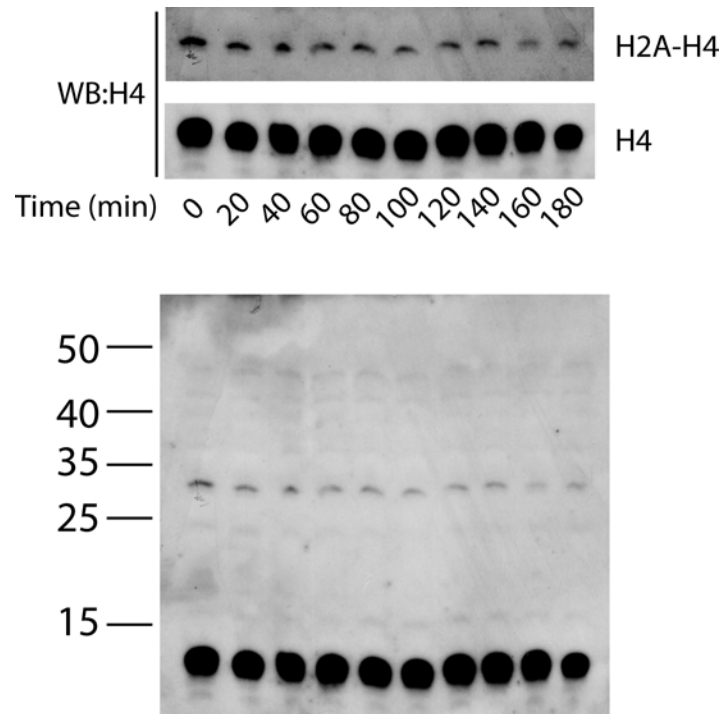


Fig. S14 Nocodazole synchronization (arrest and release) of H4 K16R mutants as in fig. S13 but analyzed using acid-extraction protocol. H4 K16R cells were arrested in metaphase with nocodazole and synchronously released. Samples were taken after release and treated with UV for 7 min on ice, and acid-extracts of isolated nuclei analyzed by SDS-PAGE and Western blot using anti-H4 antibodies.

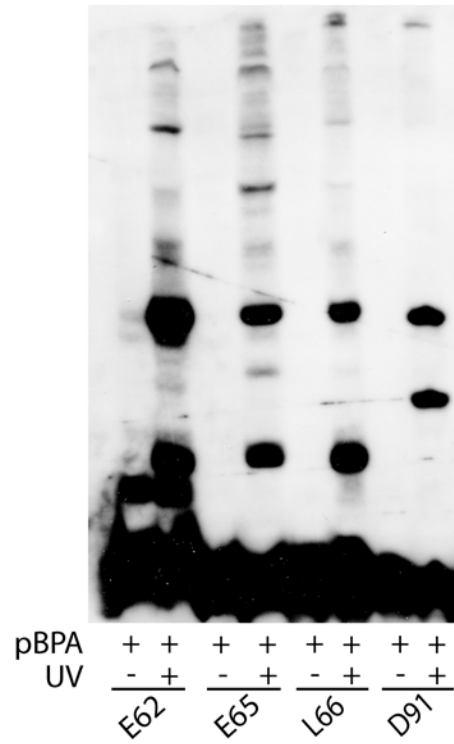


Fig. S15 Appearance of crosslinked products depends on UV irradiation. Whole cells were treated with UV for 7 min on ice. Lysates were analyzed by SDS-PAGE and Western Blot using anti-HA antibodies.

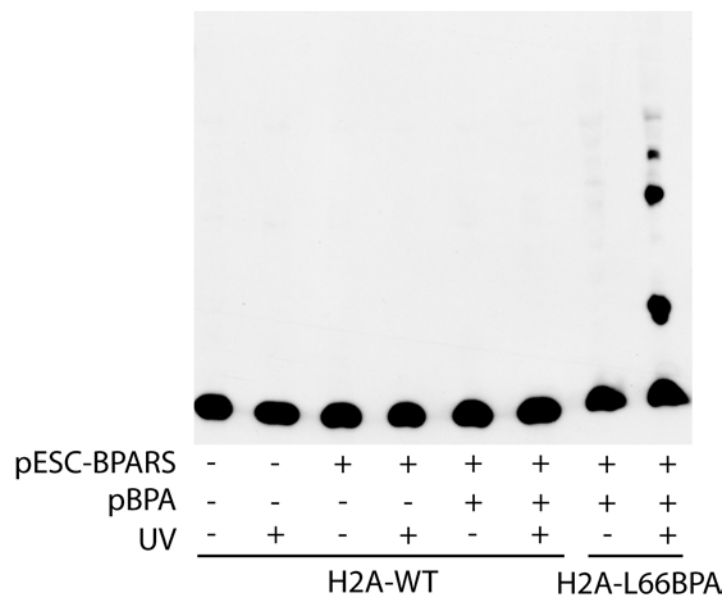


Fig. S16 Crosslinks are not a result of pBPA incorporation at genomic amber codons. Cells harboring pESC-BPARS in the presence of plasmid borne WT H2A-HA were cultured in media supplemented with/out pBPA to late exponential phase. Cells were subjected to UV irradiation, as indicated, and whole cell lysates were analyzed by SDS-PAGE and Western blot using anti-HA antibodies. This was compared to crosslinking, as described above, for an H2A containing pBPA.

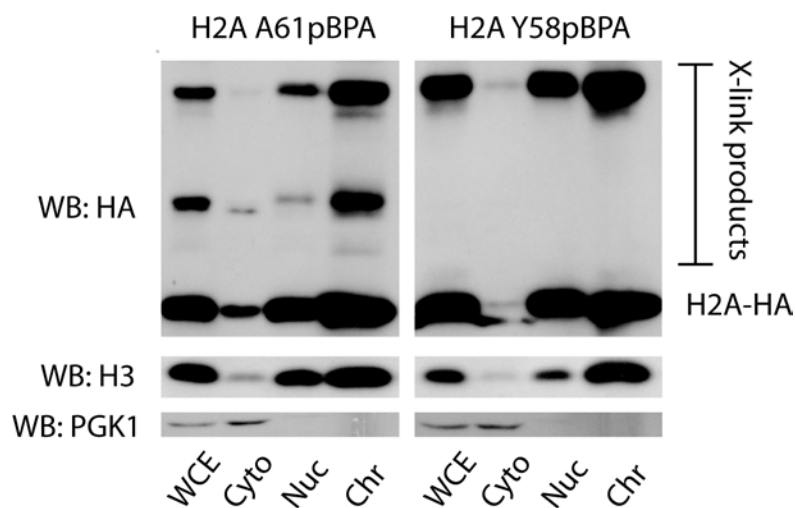


Fig. S17 Western blot analysis of subcellular fractionations for the A61pBPA and Y58pBPA crosslinked mutants. The pBPA containing histones move with the chromatin bound fractions, as do most of the H2A crosslink products, indicative of correct nucleosomal incorporation for these mutants. Controls: Histone H3 (Chromatin) and phosphoglycerate kinase 1 (PGK1, Cytosol). Abbreviations: WCE: Whole cell extract; Cyto: Cytosol; Nuc: Nuclei; Chr: Chromatin.

Table S1. Yeast Strains used in this study. Genomic mutations are highlighted for each strain.

Mutant	Strain	Genotype	Reference
	BY4741	MATa his3 Δ 1 leu2 Δ 0 met15 Δ 0 ura3 Δ 0	
<i>alk2Δ</i>	BY4741	MATa his3 Δ 1 leu2 Δ 0 met15 Δ 0 ura3 Δ 0 alk2::KanMX	(33)
<i>alk1/alk2Δ</i>	BY4741	MATa his3 Δ 1 leu2 Δ 0 met15 Δ 0 ura3 Δ 0 alk2::KanMX alk2::HIS3	this study
SIR2-GFP	BY4741	MATa his3 Δ 1 leu2 Δ 0 met15 Δ 0 ura3 Δ 0 SIR2- GFP(S65T)::HIS3	(34)
HST2-GFP	BY4741	MATa his3 Δ 1 leu2 Δ 0 met15 Δ 0 ura3 Δ 0 HST2- GFP(S65T)::HIS3	(34)
	W303	MATa leu2-3,112 trp1-1 can1-100 ura3-1 ade2-1 his3-11,15 phi+	
H3/H4 mutants		MATa his3 Δ 200 leu2 Δ 0 lys2 Δ 0 trp1 Δ 63 ura3 Δ 0 met15 Δ 0 can1::MFA1pr-HIS3 hht1-hhf1::NatMX4 hht2-hhf2::[HHTS-HHFS]-URA3	(24)
yYB3478		trp1::TetO:TRP1 lys4::LacO:LEU2 his3::LacR- GFP:HIS3 TetR-mRFP Spc42-GFP:hphNT1 ura3-52 ade2-101 leu2	(4)
yYB3675		Chr12:NAT:Chr4 Cen12::CaURA3 pGAL1:Cen4:KanMX trp1::TetO:TRP1 lys4::LacO:LEU2 his3::LacR- GFP:HIS3 TetR-mRFP Spc42-GFP:hphNT1 ura3-52 ade2-101 leu2	(4)
yYB4730		Chr12:NAT:Chr4 Cen12::CaURA3 trp1::TetO:TRP1 lys4::LacO:LEU2 his3::LacR-GFP:HIS3 TetR-mRFP Spc42- GFP:hphNT1 hht1::hht1-S10A:KanMXloxP hht2::hht2-S10A:bleloxP ura3-52 ade2-101 leu2	(4)
yYB8950		Chr12:NAT:Chr4 Cen12::CaURA3 pGAL1:Cen4:KanMX trp1::TetO:TRP1 lys4::LacO:LEU2 his3::LacR- GFP:HIS3 TetR-mRFP Spc42-GFP:hphNT1 hst2::ADE2 ura3-52 ade2-101 leu2	this study
yYB8924		Chr12:NAT:Chr4 Cen12::CaURA3 trp1::TetO:TRP1 lys4::LacO:LEU2 his3::LacR-GFP:HIS3 TetR-mRFP Spc42- GFP:hphNT1 hht1::hht1-S10A:KanMXloxP hht2::hht2-S10A:bleloxP hst2::ADE2 ura3-52 ade2-101 leu2	this study

Table S2. Primers used in this study.

Primer	Sequence (5'-3')
H2A(HTA1) -420 bp fwd	ATCAGAGCTCGCGCTGTTCCAAAATTTTCGCC
H2A(HTA1) +450 bp rev	ATCACTCGAGGCGTATATATATATACAAATATGCG
C-terminal HA tag QC fwd	GCTTCTCAAGAATTATATCCATATGATGTTCCAGATTATG CTTAAGATCGGTTCTGGTATTTTAAAG
C-terminal HA tag QC rev	CTTTAAAATACCAGAACCGATCTTAAGCATAATCTGGAAC ATCATATGGATATAATTCTTGAGAAGC
Y58TAG QC fwd	ACTTGACTGCTGTCTTGGAATAGTTGGCCGCTGAAATT
Y58TAG QC rev	TCTAAAATTTTCAGCGGCCAACTATTCCAAGACAGCAGTC
A61TAG QC fwd	CTTGGAATATTTGGCCTAGGAAATTTTAGAATTAGC
A61TAG QC rev	CAGCTAATTCTAAAATTTCTAGGCCAAATATTCCAAGAC
E65TAG QC fwd	ATTTGGCCGCTGAAATTTTATAGTTAGCTGGTAATGCTG
E65TAG QC rev	CTAGCAGCATTACCAGCTAACTATAAAATTTTCAGCGGC
alk1Δ KO fwd	GAAAAAATAACAACCTTTATCAATGTTTATTTTATTTATTA AGTATTTGATGTGAAGTAGTTTTTCTAACTATGCGGCATC AGAGC
alk1Δ KO rev	GTTTATGTATTGGAGTATACAATAGAAAGAAAATGAAAT ATAAATGTCAACATTCCTATTTGTTTTAGTGCGGTATTTC CACC

Table S3. Antibodies and dilutions applied in this study.

Company	Target	Host	Dilution
<i>Primary</i>			
Abcam (ab9110)	HA tag	Rabbit	1:10K in 3% BSA-PBS
Abcam (ab13923)	Histone H2A	Rabbit	1:2.5K in 3% Milk-TBS
Abcam (ab10158)	Histone H4	Rabbit	1:2.5K in 3% Milk-TBS
Abcam (ab7311)		Rabbit	1:500 in 3% BSA-TBS
Abcam (ab1791)	Histone H3	Rabbit	1:2.5K in 3% Milk-TBS
Active Motif (39167)	Histone H4 acetyl Lys16	Rabbit	1:2.5K in 3% Milk-TBS
Cell Signaling (9701)	Phospho-Histone H3 (Ser10)	Rabbit	1:3K in 3% BSA-TBS
Invitrogen (A6457)	Phosphoglycerate kinase1	Mouse	1:10K in 3% Milk-TBS
Santa Cruz (Sc-9996)	GFP	Mouse	1:1K in 3% Milk-TBS
<i>Secondary</i>			
Abcam (ab6721)	Rabbit	Goat	1:10K in 3% Milk-TBS
Abcam (ab6789)	Mouse	Goat	1:10K in 3% Milk-TBS

References

1. F. Mora-Bermúdez, D. Gerlich, J. Ellenberg, Maximal chromosome compaction occurs by axial shortening in anaphase and depends on Aurora kinase. *Nat. Cell Biol.* **9**, 822–831 (2007). [doi:10.1038/ncb1606](https://doi.org/10.1038/ncb1606) [Medline](#)
2. P. Vagnarelli, S. Ribeiro, L. Sennels, L. Sanchez-Pulido, F. de Lima Alves, T. Verheyen, D. A. Kelly, C. P. Ponting, J. Rappsilber, W. C. Earnshaw, Repo-Man coordinates chromosomal reorganization with nuclear envelope reassembly during mitotic exit. *Dev. Cell* **21**, 328–342 (2011). [doi:10.1016/j.devcel.2011.06.020](https://doi.org/10.1016/j.devcel.2011.06.020) [Medline](#)
3. M. J. Hendzel, Y. Wei, M. A. Mancini, A. Van Hooser, T. Ranalli, B. R. Brinkley, D. P. Bazett-Jones, C. D. Allis, Mitosis-specific phosphorylation of histone H3 initiates primarily within pericentromeric heterochromatin during G₂ and spreads in an ordered fashion coincident with mitotic chromosome condensation. *Chromosoma* **106**, 348–360 (1997). [doi:10.1007/s004120050256](https://doi.org/10.1007/s004120050256) [Medline](#)
4. G. Neurohr, A. Naegeli, I. Titos, D. Theler, B. Greber, J. Díez, T. Gabaldón, M. Mendoza, Y. Barral, A midzone-based ruler adjusts chromosome compaction to anaphase spindle length. *Science* **332**, 465–468 (2011). [doi:10.1126/science.1201578](https://doi.org/10.1126/science.1201578) [Medline](#)
5. P. J. Robinson, W. An, A. Routh, F. Martino, L. Chapman, R. G. Roeder, D. Rhodes, 30 nm chromatin fibre decompaction requires both H4-K16 acetylation and linker histone eviction. *J. Mol. Biol.* **381**, 816–825 (2008). [doi:10.1016/j.jmb.2008.04.050](https://doi.org/10.1016/j.jmb.2008.04.050) [Medline](#)
6. M. Shogren-Knaak, H. Ishii, J. M. Sun, M. J. Pazin, J. R. Davie, C. L. Peterson, Histone H4-K16 acetylation controls chromatin structure and protein interactions. *Science* **311**, 844–847 (2006). [doi:10.1126/science.1124000](https://doi.org/10.1126/science.1124000) [Medline](#)
7. C. J. Fry, M. A. Shogren-Knaak, C. L. Peterson, Histone H3 amino-terminal tail phosphorylation and acetylation: Synergistic or independent transcriptional regulatory marks? *Cold Spring Harb. Symp. Quant. Biol.* **69**, 219–226 (2004). [doi:10.1101/sqb.2004.69.219](https://doi.org/10.1101/sqb.2004.69.219)
8. F. Gordon, K. Luger, J. C. Hansen, The core histone N-terminal tail domains function independently and additively during salt-dependent oligomerization of nucleosomal arrays. *J. Biol. Chem.* **280**, 33701–33706 (2005). [doi:10.1074/jbc.M507048200](https://doi.org/10.1074/jbc.M507048200) [Medline](#)

9. B. Dorigo, T. Schalch, A. Kulangara, S. Duda, R. R. Schroeder, T. J. Richmond, Nucleosome arrays reveal the two-start organization of the chromatin fiber. *Science* **306**, 1571–1573 (2004). [doi:10.1126/science.1103124](https://doi.org/10.1126/science.1103124) [Medline](#)
10. D. Sinha, M. A. Shogren-Knaak, Role of direct interactions between the histone H4 tail and the H2A core in long range nucleosome contacts. *J. Biol. Chem.* **285**, 16572–16581 (2010). [doi:10.1074/jbc.M109.091298](https://doi.org/10.1074/jbc.M109.091298) [Medline](#)
11. L. M. Johnson, P. S. Kayne, E. S. Kahn, M. Grunstein, Genetic evidence for an interaction between SIR3 and histone H4 in the repression of the silent mating loci in *Saccharomyces cerevisiae*. *Proc. Natl. Acad. Sci. U.S.A.* **87**, 6286–6290 (1990). [doi:10.1073/pnas.87.16.6286](https://doi.org/10.1073/pnas.87.16.6286) [Medline](#)
12. E. C. Park, J. W. Szostak, Point mutations in the yeast histone H4 gene prevent silencing of the silent mating type locus HML. *Mol. Cell. Biol.* **10**, 4932–4934 (1990). [Medline](#)
13. L. Davis, J. W. Chin, Designer proteins: Applications of genetic code expansion in cell biology. *Nat. Rev. Mol. Cell Biol.* **13**, 168–182 (2012). [Medline](#)
14. H. Neumann, Rewiring translation—Genetic code expansion and its applications. *FEBS Lett.* **586**, 2057–2064 (2012). [doi:10.1016/j.febslet.2012.02.002](https://doi.org/10.1016/j.febslet.2012.02.002) [Medline](#)
15. J. W. Chin, T. A. Cropp, J. C. Anderson, M. Mukherji, Z. Zhang, P. G. Schultz, An expanded eukaryotic genetic code. *Science* **301**, 964–967 (2003). [doi:10.1126/science.1084772](https://doi.org/10.1126/science.1084772) [Medline](#)
16. K. Luger, A. W. Mäder, R. K. Richmond, D. F. Sargent, T. J. Richmond, Crystal structure of the nucleosome core particle at 2.8 Å resolution. *Nature* **389**, 251–260 (1997). [doi:10.1038/38444](https://doi.org/10.1038/38444) [Medline](#)
17. A. E. Kelly, C. Ghenoïu, J. Z. Xue, C. Zierhut, H. Kimura, H. Funabiki, Survivin reads phosphorylated histone H3 threonine 3 to activate the mitotic kinase Aurora B. *Science* **330**, 235–239 (2010). [doi:10.1126/science.1189505](https://doi.org/10.1126/science.1189505) [Medline](#)
18. F. Wang, J. Dai, J. R. Daum, E. Niedzialkowska, B. Banerjee, P. T. Stukenberg, G. J. Gorbsky, J. M. Higgins, Histone H3 Thr-3 phosphorylation by Haspin positions Aurora B at centromeres in mitosis. *Science* **330**, 231–235 (2010). [doi:10.1126/science.1189435](https://doi.org/10.1126/science.1189435) [Medline](#)

19. Y. Yamagishi, T. Honda, Y. Tanno, Y. Watanabe, Two histone marks establish the inner centromere and chromosome bi-orientation. *Science* **330**, 239–243 (2010).
[doi:10.1126/science.1194498](https://doi.org/10.1126/science.1194498) [Medline](#)
20. C. S. Campbell, A. Desai, Tension sensing by Aurora B kinase is independent of survivin-based centromere localization. *Nature* **497**, 118–121 (2013). [doi:10.1038/nature12057](https://doi.org/10.1038/nature12057) [Medline](#)
21. K. K. Adhvaryu, E. Berge, H. Tamaru, M. Freitag, E. U. Selker, Substitutions in the amino-terminal tail of *Neurospora* histone H3 have varied effects on DNA methylation. *PLOS Genet.* **7**, e1002423 (2011). [doi:10.1371/journal.pgen.1002423](https://doi.org/10.1371/journal.pgen.1002423) [Medline](#)
22. B. G. Mellone, L. Ball, N. Suka, M. R. Grunstein, J. F. Partridge, R. C. Allshire, Centromere silencing and function in fission yeast is governed by the amino terminus of histone H3. *Curr. Biol.* **13**, 1748–1757 (2003). [doi:10.1016/j.cub.2003.09.031](https://doi.org/10.1016/j.cub.2003.09.031) [Medline](#)
23. Y. Wei, L. Yu, J. Bowen, M. A. Gorovsky, C. D. Allis, Phosphorylation of histone H3 is required for proper chromosome condensation and segregation. *Cell* **97**, 99–109 (1999).
[doi:10.1016/S0092-8674\(00\)80718-7](https://doi.org/10.1016/S0092-8674(00)80718-7) [Medline](#)
24. J. Dai, E. M. Hyland, D. S. Yuan, H. Huang, J. S. Bader, J. D. Boeke, Probing nucleosome function: a highly versatile library of synthetic histone H3 and H4 mutants. *Cell* **134**, 1066–1078 (2008). [doi:10.1016/j.cell.2008.07.019](https://doi.org/10.1016/j.cell.2008.07.019) [Medline](#)
25. P. Vagnarelli, D. F. Hudson, S. A. Ribeiro, L. Trinkle-Mulcahy, J. M. Spence, F. Lai, C. J. Farr, A. I. Lamond, W. C. Earnshaw, Condensin and Repo-Man-PP1 co-operate in the regulation of chromosome architecture during mitosis. *Nat. Cell Biol.* **8**, 1133–1142 (2006). [doi:10.1038/ncb1475](https://doi.org/10.1038/ncb1475) [Medline](#)
26. J. Y. Hsu, Z. W. Sun, X. Li, M. Reuben, K. Tatchell, D. K. Bishop, J. M. Grushcow, C. J. Brame, J. A. Caldwell, D. F. Hunt, R. Lin, M. M. Smith, C. D. Allis, Mitotic phosphorylation of histone H3 is governed by Ipl1/aurora kinase and Glc7/PP1 phosphatase in budding yeast and nematodes. *Cell* **102**, 279–291 (2000).
[doi:10.1016/S0092-8674\(00\)00034-9](https://doi.org/10.1016/S0092-8674(00)00034-9) [Medline](#)

27. D. Mumberg, R. Müller, M. Funk, Regulatable promoters of *Saccharomyces cerevisiae*: Comparison of transcriptional activity and their use for heterologous expression. *Nucleic Acids Res.* **22**, 5767–5768 (1994). [doi:10.1093/nar/22.25.5767](https://doi.org/10.1093/nar/22.25.5767) [Medline](#)
28. Y. Ryu, P. G. Schultz, Efficient incorporation of unnatural amino acids into proteins in *Escherichia coli*. *Nat. Methods* **3**, 263–265 (2006). [doi:10.1038/nmeth864](https://doi.org/10.1038/nmeth864) [Medline](#)
29. H. Neumann, S. M. Hancock, R. Buning, A. Routh, L. Chapman, J. Somers, T. Owen-Hughes, J. van Noort, D. Rhodes, J. W. Chin, A method for genetically installing site-specific acetylation in recombinant histones defines the effects of H3 K56 acetylation. *Mol. Cell* **36**, 153–163 (2009). [doi:10.1016/j.molcel.2009.07.027](https://doi.org/10.1016/j.molcel.2009.07.027) [Medline](#)
30. M. C. Keogh, T. A. Mennella, C. Sawa, S. Berthelet, N. J. Krogan, A. Wolek, V. Podolny, L. R. Carpenter, J. F. Greenblatt, K. Baetz, S. Buratowski, The *Saccharomyces cerevisiae* histone H2A variant Htz1 is acetylated by NuA4. *Genes Dev.* **20**, 660–665 (2006). [doi:10.1101/gad.1388106](https://doi.org/10.1101/gad.1388106) [Medline](#)
31. S. B. Haase, *Curr. Protoc. Cytom.* Chapter 7, Unit 7 23 (2004).
32. D. Shechter, H. L. Dormann, C. D. Allis, S. B. Hake, Extraction, purification and analysis of histones. *Nat. Protoc.* **2**, 1445–1457 (2007). [doi:10.1038/nprot.2007.202](https://doi.org/10.1038/nprot.2007.202) [Medline](#)
33. C. B. Brachmann, A. Davies, G. J. Cost, E. Caputo, J. Li, P. Hieter, J. D. Boeke, Designer deletion strains derived from *Saccharomyces cerevisiae* S288C: A useful set of strains and plasmids for PCR-mediated gene disruption and other applications. *Yeast* **14**, 115–132 (1998). [doi:10.1002/\(SICI\)1097-0061\(19980130\)14:2<115::AID-YEA204>3.0.CO;2-2](https://doi.org/10.1002/(SICI)1097-0061(19980130)14:2<115::AID-YEA204>3.0.CO;2-2) [Medline](#)
34. W. K. Huh, J. V. Falvo, L. C. Gerke, A. S. Carroll, R. W. Howson, J. S. Weissman, E. K. O'Shea, Global analysis of protein localization in budding yeast. *Nature* **425**, 686–691 (2003). [doi:10.1038/nature02026](https://doi.org/10.1038/nature02026) [Medline](#)